Analytical Methods

Accepted Manuscript

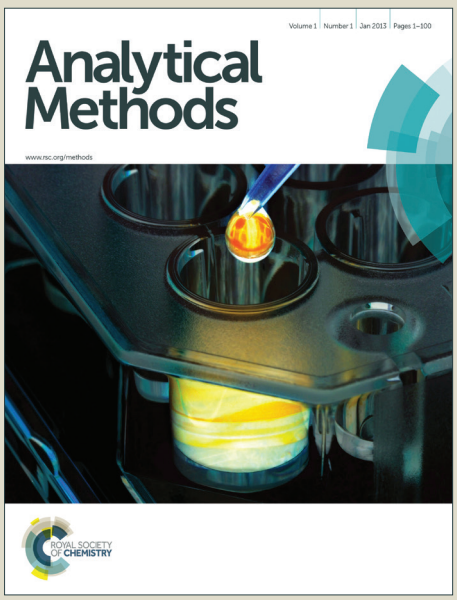

ROYAL SOCIETY OF CHEMISTRY

www.rsc.org/methods

Cite this: DOI: 10.1039/c0xx00000x

www.rsc.org/xxxxxx

ARTICLE TYPE

One-pot Synthesis of Dual-emitting BSA-Pt-Au Bimetallic Nanoclusters for Fluorescence Ratio-metric Detection of Mercury Ions and Cysteine

Shou-Nian Ding* and Yun-Xia Guo

Received (in XXX, XXX) Xth XXXXXXXXX 20XX, Accepted Xth XXXXXXXXX 20XX

DOI: 10.1039/b000000x

Water-soluble and dual-emitting bovine serum albumin-templated bimetallic platinum-gold fluorescent nanoclusters (BSA-Pt-Au NCs) have been firstly synthesized by a simple and rapid one-pot synthesis strategy at a vital molar ratio of Pt/Au precursors under basic conditions. The BSA-Pt-Au NCs show unique and well-resolved dual-emission bands at 405 nm and 640 nm corresponding to the emission of BSA-metal complex and Au NCs under the excitation at 340 nm, respectively. Interestingly, with the addition of mercury (II) (Hg^{2+}) ions, the emission intensity at 405 nm (F_{405}) has a negligible influence, while the emission intensity at 640 nm (F_{640}) decreases dramatically, which is due to the specific and strong d^{10}-d^{10} interaction between Hg^{2+} ions and Au atoms/ions on the surface of the BSA-Pt-Au NCs. Meanwhile, cysteine (Cys) could effectively block Hg^{2+} ions to quench the fluorescence of BSA-Pt-Au NCs, which is based on the strong interaction between Hg^{2+} ions and thiol functional group. These allowed the analysis of Hg^{2+} ions and Cys with the ratio of two emission intensities (F_{405}/F_{640}) in ultra-sensitivity and selectivity with high accuracy. The limit of detection (LOD) was 0.3 nM for Hg^{2+} ions and 0.04 μM for Cys (S/N=3), respectively. This work indicates that the fluorescent sensor possess potential applications for biological detection.

Introduction

Heavy metal ions, even at very low concentrations, have some negative effects on the environment and cause severe medical threats to human health.[1] For example, mercury(II) (Hg^{2+}) ions, one of the most omnipresent pollutants released from natural operations and human activities, have long-term adverse influences on kidney, liver, vision problems, deafness, losses of muscle coordination, the central nervous systems, and so forth.[2-5] Therefore, it is extremely significant to develop a simple and rapid method to detect Hg^{2+} ions with high sensitivity and selectivity. During the past decades, various techniques have been designed for monitoring Hg^{2+} ions, including atomic absorption spectrometry, electrochemical sensors, colorimetric assays and inductively coupled plasma mass spectrometry.[6-10] However, most of them have some defects, such as time-consuming, complicated procedures, specialized skills needed and sophisticated instrumentation. To overcome these drawbacks, fluorescent noble metal nanoclusters, owing to their operational simplicity, cost-effectiveness, easy visualization and high sensitivity,[11-14] have been widely used to develop a new platform for detecting Hg^{2+} ions.

Cysteine (Cys), the only one containing a free thiol moiety among numerous amino acids, plays an important role in maintaining the physiological redox homeostasis by the mutual transformation between free thiols and disulfides in vivo.[15] Altered levels of the Cys could cause some pathological problems, including Alzheimer's and Parkinson's diseases.[16] Consequently, developing a relatively inexpensive, reliable and rapid methods for the analysis of Cys is particular interest and crucial. In recent years, many methods, including high-performance liquid chromatography,[17] capillary electrophoresis[18] and mass spectrometry,[19] have been used to detect Cys. Nevertheless, some limitations such as the need for sophisticated instrumentation, technical expertise and long analysis times have been emerged in an endless stream. In order to develop the alternative approaches avoiding these drawbacks, growing interest has focused on fluorescence-based strategies, owing to their intrinsically high sensitivity and ease of operation.

Nowadays, noble metal nanoclusters containing several to tens of atoms, like gold nanoclusters (Au NCs), have been comprehensive applied to detect heavy metal ions, protein and DNA. Au NCs, compared with traditional fluorescent quantum dots (CdS, CdSe and ZnS) and fluorescent dyes, possess the advantages of ultra-small size, good photostability and biocompatibility, which makes them have more promising applications as optical probes in sensing and bioimaging.[20, 21] Until now, several methods have been used to synthesize these highly fluorescent Au NCs, such as etching method and high-temperature splitting method. However, one-pot heating approach

Jiangsu Province Hi-Tech Key Laboratory for Bio-medical Research, School of Chemistry and Chemical Engineering, Southeast University, Nanjing 211189, China.
E-mail: snding@seu.edu.cn); Fax/Tel: +86- 25-52090621

by biological protein macromolecules as stabilizing and reducing agent at basic conditions, including bovine serum albumin,[22] lysozyme[23] and lactoferrin[24] is more popular in recent years. Among them, BSA-Au NCs possess higher quantum yield than lysozyme or lactoferrin-Au NCs. Although a number of Au NCs fluorescent sensors have been devised to monitor Hg^{2+} ions (Cys) based on the fluorescence intensity change, their obtained signal output was easily influenced by the probe concentration, photo bleaching, even the light source stability and so forth. These problems could be circumvented by the ratio-metric fluorescence technique.[25] Therefore, developing the fluorescence probes with intrinsic dual-emitting optical properties and low toxicity via a simple preparation method is much desirable for wide applications of ratio-metric fluorescence measurement.

Herein, as a new alloy material, the bimetallic and dual-emission BSA-Pt-Au NCs fluorescent nanoprobes with prominent fluorescence properties, good dispersibility, and easy water solubility were successfully synthesized for the first time by a one-pot synthetic strategy with the template of BSA as both stabilizing and reducing agent. The obtained BSA-Pt-Au NCs possess two apparent emission bands centered at 405 and 640 nm, respectively, corresponding to BSA-Pt and Au complexes emission and Au NCs emission. The fluorescence of BSA-Pt-Au NCs could be observably quenched by Hg^{2+} ions due to the d^{10}-d^{10} metallophilic interaction between Au^{+} ($4f^{14}5d^{10}$) and Hg^{2+} ($4f^{14}5d^{10}$).[26, 27] However, the "off" fluorescence of BSA-Pt-Au NCs by Hg^{2+} ions is inhibited in presence of Cys based on the strong interaction between Hg^{2+} ions and thiol functional group of the Cys (Cys-Hg^{2+}-Cys). Accordingly, the ratio-metric fluorescence sensor has been applied to detect Hg^{2+} ions and Cys in aqueous solution and real samples. The principle of sensing concept is shown in Scheme 1. To the best of our knowledge, this is the first example to construct a ratio-metric fluorescence sensing platform for Hg^{2+} ions and Cys based on highly efficient dual-emitting fluorescent BSA-Pt-Au NCs.

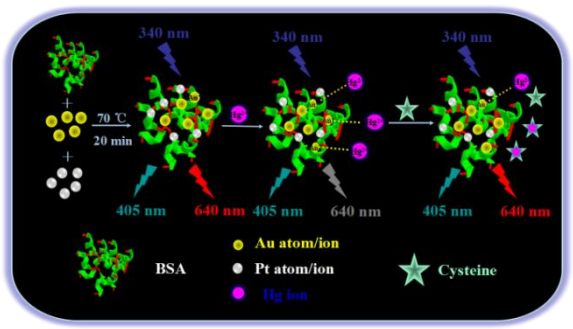

Scheme 1 Schematic representation of ratio-metric fluorescence detection of Hg^{2+} ions and cysteine by dual-emitting BSA-Pt-Au NCs.

Experimental Section

Materials and Apparatus

Bovine serum albumin (BSA) was purchased from Shanghai Sangon Biological Co. Ltd. (Shanghai, China). Hydrogen tetrachloroaurate trihydrate ($HAuCl_4.3H_2O$, >99.9%) was obtained from Shanghai Sinopharm Chemical Reagent Co. Ltd. (Shanghai, China). Chloroplatinic acid (H_2PtCl_6, >99.9%) and 4-(2-hydroxyethyl) piperazine-1-ethanesulfonic acid (HEPES) were purchased from from Sigma-aldrich Co. Ltd. Mercuric nitrate ($Hg(NO_3)_2$) was purchased from Taixing Chemical Reagent Co. Ltd. (Jiangsu, China). Cysteine (Cys, 99%) was purchased from Adamas-beta Inc. (Shanghai, China). All other chemicals were of analytical grade and used without further purification. The water used throughout all the experiments was puried through a Millipore system. Transmission electron microscopy (TEM) and high resolution transmission electron microscopy (HRTEM) images were obtained on a JEM-2100 transmission electron microscope (JEOL Ltd.). UV-vis absorption spectra were recorded on a Shimadzu UV-2450 spectrophotometer (Tokyo, Japan). The fluorescence measurements were performed on a Fluoromax-4 fluorescence spectrofluorometer (Horiba, USA). Energy-dispersive X-ray spectroscopy (EDS) was carried out using a FEI Sirion 200 scanning electron microscope (FEI). The fluorescent lifetime measurements were performed on an FL-TCSPC fluorescence spectrophotometer (Horiba Jobin Yvon, USA).

One-pot Preparation of Fluorescent BSA-Pt-Au NCs

All glass were used in the experiments were cleaned by the freshly prepared aqua regia ($HCl:HNO_3$ volume ratio = 3:1), and rinsed thoroughly in water prior to use. The BSA-Pt-Au NCs were synthesized by reduction of $HAuCl_4$ and H_2PtCl_6 using BSA as both reducing agent and capping agent in alkaline conditions. In a typical experiment, 5.0 mL solution containing BSA (50 mg mL^{-1}), $HAuCl_4$ (10 mM), H_2PtCl_6 (1.0 mM) and NaOH (100 mM) in a 25 mL round bottom flask was incubated at 70 ℃ for 20 min and then cooled down to room temperature. During the whole process, the color of the solution changed from light yellow to pale brown. To obtain the pure BSA-Pt-Au NCs, the solution was subjected to dialysis against double distilled water through a 3.5 kDa molecular weight cutoff membrane for 24 hours. Similarly, the BSA-Pt-Au NCs with different molar ratio of Pt/Au precursors, BSA-Pt NCs and BSA-Au NCs were obtained through the same synthesis and purification processes.

Optimizing Experimental Conditions

In order to obtain a highly sensitive response for the detection of Hg^{2+} ions and Cys, the optimization of the different pH values of HEPES solutions were carried out in our experiment. Briefly, 10 μL of BSA-Pt-Au NCs (20 mg mL^{-1}) were added into 250 μL of HEPES solutions (50 mM) with different pH values and incubated for 30 min, then 240 μL of double distilled water was added into the above mixed solution. All the excitation wavelengths and the excitation/emission slit widths were set at 340 nm and 5 nm, respectively.

Fluorescence Assay of Hg^{2+} Ions

In a typical run, various concentrations of Hg^{2+} ions were mixed with 10 μL of BSA-Pt-Au NCs (20 mg mL^{-1}) in a 250 μL HEPES solution (pH 8.0, 50 mM) for a few seconds. And the final volume of the mixtures was adjusted to 500 μL with double distilled water. Then all the mixtures were equilibrated at room temperature for 30 min before the fluorescence measurements.

Fluorescence Detection of Cysteine

Various concentrations of Cys were mixed with 22 μM Hg^{2+} ions

by a vortex mixer for ten minutes, and then added into the 10 μL of BSA-Pt-Au NCs (20 mg mL^{-1}) in a 250 μL HEPES solution (pH 8.0, 50 mM), after that the final volume of the mixtures was adjusted to 500 μL with double distilled water.

Measurement of Fluorescence Lifetimes

The fluorescence lifetimes of BSA-Pt-Au NCs in the absence and presence of Hg^{2+} ions were measured on the FL-TCSPC fluorescence spectrophotometer using the luminescence decay mode. The complex was excited with a flash of the xenon lamp at 280 nm and the emission wavelength at 640 nm, and the fluorescence decay was subsequently recorded.

Sensor Selectivity Investigation

In order to evaluate the selectivity of the fluorescence sensor for Hg^{2+} ions and Cys, a series of different metal ions, including Cd^{2+}, K^{+}, Fe^{3+}, Mg^{2+}, Ca^{2+}, Ni^{2+}, Fe^{2+}, Sn^{2+}, Zn^{2+}, Cu^{2+}, Cr^{3+}, Sr^{2+}, Pb^{2+}, Mn^{2+}, Co^{2+}, Ba^{2+}, Ag^{+} ions and the mixtures of 22 μM Hg^{2+} ions with various kinds of amino acids were poured into the solution of 10 μL BSA-Pt-Au NCs (20 mg mL^{-1}) and 250 μL HEPES (pH 8.0, 50 mM) under the same conditions, respectively. The final volume of the mixture was adjusted to 500 μL with double distilled water. The concentrations of Hg^{2+} ions and Cys were 22 μM and 50 μM, however, the concentrations of all other interference metal ions and amino acids were 50 μM and 200 μM, respectively.

Real Samples

The urine and serum samples were obtained from the Southeast University Affiliated Zhongda Hospital. Each sample was diluted with HEPES buffer solution (pH 8.0) by 10-fold for subsequent analysis.

Results and Discussion

Synthesis and Characterization of BSA-Pt-Au NCs

The BSA-Pt-Au NCs was synthesized by reducing $HAuCl_4$ and H_2PtCl_6 using BSA as both reducing agent and capping agent under basic conditions for 20 min at 70 ℃. The optical properties of the BSA-Pt-Au NCs were characterized by the UV-vis absorption and fluorescence spectroscopy (as shown in Fig. 1A). The UV-vis absorption spectrum of the BSA-Pt-Au NCs in aqueous solution has an obvious peak at about 275 nm which is attributed to the absorption of BSA biomolecules. Furthermore, the UV-vis absorption spectrum shows no obvious local surface plasmon resonance adsorption over the Au nanoparticles absorbance range, which suggests that highly purified BSA-Pt-Au NCs have been obtained without the formation of larger Au NPs due to the absent peak of gold nanoparticles around 520 nm.[28] The as-synthesized pale brown BSA-Pt-Au NCs solution (under visible light) emits intense red luminescence under UV light (365 nm), which can be clearly observed by naked eyes (as shown in the inset of Fig. 1A). Meanwhile, the fluorescence spectrum of BSA-Pt-Au NCs displays two peaks centered at 405 nm and 640 nm, which maybe correspond to the BSA-Pt/Au complexes and Au NCs, respectively.[29] To demonstrate the emission peak at 405 nm, the fluorescence spectra of the BSA-Pt-Au NCs, BSA-Au NCs, BSA-Pt complexes and BSA were measured, as shown in Fig. 1C. The BSA possess a relatively weak peak at 405 nm, which is most likely to originate from dityrosine-like fluorescence reported by Huggins et al..[30] However, BSA-Pt complex also has one peak at 405 nm and the intensity is much lower than that of BSA-Pt-Au NCs at the same concentration. Furthermore, the intensity ratio of the two peaks (F_{405}/F_{640}) at BSA-Pt-Au NCs was 2:1 while the ratio was 1:1 at BSA-Au NCs. The reason is of forming BSA-Pt or BSA-Au complexes, which could be enhancing the fluorescent intensity of BSA due to the increasing structural rigidity of BSA and the synergistic effect between Au and Pt for BSA. Therefore, the peak at 405 nm should be assigned to the emission of BSA-Pt and BSA-Au complexes. To obtain the morphology and size of the prepared BSA-Pt-Au NCs, TEM and HRTEM were performed. As shown in Fig. S1 (Supporting Information), the BSA-Pt-Au NCs were nearly spherical and well-separated with the average diameter about 2 nm, and Pt is doped in the BSA-Pt-Au NCs, which is proven by the EDS experiment. The Fig. 1B shows the dual-emitting fluorescence spectra of the BSA-Pt-Au NCs at 405 nm and 640 nm with the excitation wavelengths varying from 320 nm to 350 nm. The emission intensity at 405 nm increased in the excitation range of 320 - 340 nm and then decreased gradually, but the maximum emission peak at 640 nm was observed independent with the excitation wavelength range. Thus, the excitation wavelength of 340 nm was chosen for next fluorescence measurements. The formation of the fluorescent BSA-Pt-Au NCs was also confirmed by EDS, as shown in Fig. 1D. The EDS spectrum shows the peaks corresponding to C, N, O, S elements, which maybe originates from BSA, and the existence of Pt and Au element proves the successful synthesis of BSA-Pt-Au NCs by this method.

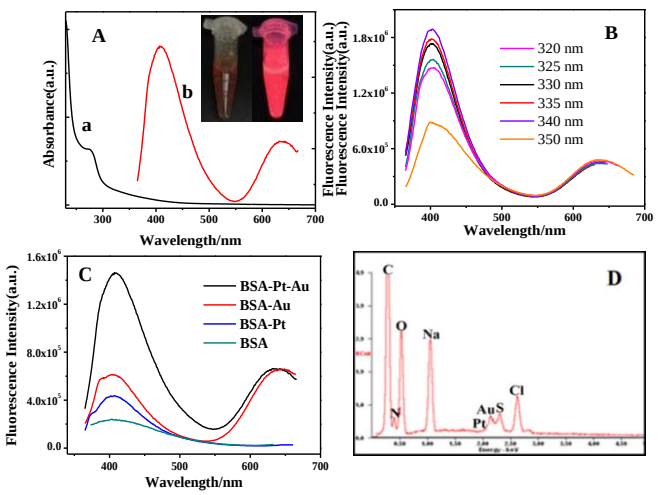

Fig. 1 (A) UV-vis absorption (a) and emission (b) spectra of the as-prepared BSA-Pt-Au NCs. The inset shows the corresponding photographs of BSA-Pt-Au NCs in aqueous solution under visible light (left) and 365 nm UV light (right), respectively. (B) Fluorescence emission spectra of BSA-Pt-Au NCs at different excitation wavelengths varying from 320 to 350 nm. (C) Fluorescence emission spectra of the BSA-Pt-Au NCs, BSA-Au NCs, BSA-Pt complexes and BSA at excitation wavelength 340 nm. (D) The EDS of the fluorescent BSA-Pt-Au NCs.

Mechanism of Detection of Hg^{2+} Ions and Cysteine

The feasibility of using such probe for Hg^{2+} ions and cysteine (Cys) detection was explored. The solution of BSA-Pt-Au NCs exhibited a relatively strong fluorescence peak at 405 and 640 nm (curve a in the Fig. 2), but a significant fluorescence quenching was observed after the addition of Hg^{2+} ions into the BSA-Pt-Au NCs solution (Fig. 2, curve b), however, the quenching phenomenon does not occur when the Hg^{2+} ions and Cys exist in the BSA-Pt-Au NCs solution at the same time(Fig. 2, curve c), furthermore, the fluorescence "turn-off-on" effect can be observed visually in the inset of Fig. 2, which proved that our bimetallic fluorescence sensor could effectively test Hg^{2+} ions and Cys. It is also worth noting that the fluorescence intensity at 405 nm of the bimetallic BSA-Pt-Au NCs has a little change upon increasing the concentration of Hg^{2+} ions from 0 to 22 μM and Cys from 0.1 μM to 50 μM, yet the fluorescent intensity of 640 nm wavelength dramatically decreased/increased (Fig. 5A, 5C). Therefore, the most probable explanation for the quenching of fluorescence of BSA-Pt-Au NCs in the presence of Hg^{2+} ions is based on the d^{10}-d^{10} metallophilic interaction between Au^{+} and Hg^{2+} (Au^{+}-Hg^{2+}).[26, 27] Moreover, Cys could block the combination of Au^{+}-Hg^{2+} by interacting with thiophilic Hg^{2+} ions through formation of stable S-Hg^{2+} bonds.[31]

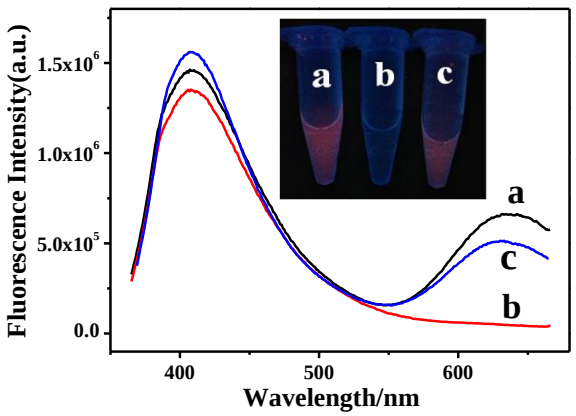

Fig. 2 Fluorescence emission spectra of BSA-Pt-Au NCs (a), after adding 22 μM Hg^{2+} ions (b) and 22 μM Hg^{2+} ions with 50 μM cysteine (c) at the excitation wavelength of 340 nm. The inset shows the corresponding photographs of BSA-Pt-Au NCs without (a), with 22 μM Hg^{2+} ions (b) and 22 μM Hg^{2+} ions with 50 μM cysteine (c) under 365 nm light, respectively.

In order to further explain the mechanism of the quenching BSA-Pt-Au NCs by Hg^{2+} ions, the time-resolved fluorescence of the BSA-Pt-Au NCs and the BSA-Pt-Au NCs/Hg^{2+} metal complexes were studied. Due to differences in the distribution of complex luminescent pathways resulting from multiple BSA-Pt-Au NCs species and/or sites,[32] the fluorescence intensity of BSA-Pt-Au NCs follows dual-exponential decay kinetics (Fig. S2, Supporting Information). Table 1 shows that the BSA-Pt-Au NCs have two fluorescence lifetimes, which is similar with the results reported by Chen et al..[29] However, the values are much shorter than the fluorescence lifetime of the BSA-Au clusters reported by Raut et al.,[33] which is likely due to the difference of synthetic materials and temperature. From the Table 1, it is found that the fluorescence lifetimes of the BSA-Pt-Au NCs have a little change with the addition of Hg^{2+} ions, which indicates that the turn off fluorescence maybe obeys a simple static quenching mechanism.[34]

Table 1. Fluorescent lifetimes of the BSA-Pt-Au NCs and the BSA-Pt-Au NC/Hg^{2+}. BSA-Pt-Au NCs, 400 μg mL^{-1}, Hg^{2+} ions, 22 μM.

Sample	τ_1/ns (%)	τ_2/ns (%)
BSA-Pt-Au CNs	1.28 (48.36)	5.14 (51.64)
BSA-Pt-Au CNs/Hg^{2+}	1.10 (45.22)	4.41 (54.78)
Excitation: 280nm; Emission wavelength: 640 nm		

Optimization of the Experimental Conditions

In order to obtain the strong fluorescent products, the amounts of BSA, the molar ratio of Pt/Au precursors, and the pH of the solutions were considered in our experiment. BSA macromolecules as both reducing agent and capping agent for the formation of the fluorescent BSA-Pt-Au NCs, the fluorescence intensity of the BSA-Pt-Au NCs increases with the BSA concentration and plateaus beyond 50 mg mL^{-1} (the data not shown). Thus, the concentration of BSA was fixed at 50 mg mL^{-1}. The composition of Pt and Au must be important factors on the fluorescence of BSA-Pt-Au NCs, Fig. S3 (Supporting Information) shows that the optimal molar ratios of Pt/Au is 1:10. Owing to the pH of the reaction solution could greatly affect the fluorescence intensity of bimetallic BSA-Pt-Au NCs and the reaction between Hg^{2+} ions and Cys. Thus, the fluorescence intensity of the prepared bimetallic BSA-Pt-Au NCs in the HEPES buffer solutions at different pH from 5.0 to 12.0 was studied, as shown in Fig. 3A and 3B. Although the maximum ratio of two emission intensity (F_{405}/F_{640}) was obtained in the pH 9.0 buffer solution, yet, considering the fluorescence stability, metal ions properties, sewage discharge standards and pKa of Cys for pH value of the solution, pH 8.0 was chosen as the optimum condition in the experiment.

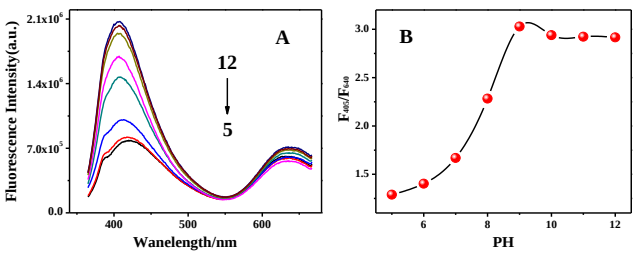

Fig. 3 (A) Effects of pH values (from 5 to 12) on the fluorescence of BSA-Pt-Au NCs; (B) The corresponding fluorescence intensity ratios (F_{405}/F_{640}) of BSA-Pt-Au NCs at various pH values.

Detection of Hg^{2+} Ions and Cysteine

The strong binding energies of Hg^{2+} with Au^{+} and the interaction between Hg^{2+} ions and thiol functional group of Cys make this method highly sensitive. When aliquots of Hg^{2+} ions solution was successively added to the BSA-Pt-Au NCs solution, the fluorescence intensity decreased gradually and appeared little blue shift phenomenon maybe rise from the formation of the metal complex.[35, 36] From the Fig. 4A, the intensity of the

fluorescence decreased gradually with the increasing concentrations of Hg^{2+} ions, and the relationship between the ratio of two emission intensity (F_{405}/F_{640}) and the concentration of Hg^{2+} ions was in the range of 0.5 nM - 22 μM with the limit of detection for Hg^{2+} ions(Fig. 4B), at a signal-to-noise ratio of 3, was estimated to be 0.3 nM, which was much lower than the maximum level of Hg^{2+} ions in drinking water permitted by the United States Environmental Protection Agency (EPA).[37] Similarly, When 22 μM Hg^{2+} ions and different concentrations of Cys mixed solutions were added into the BSA-Pt-Au NCs, the fluorescence intensity increased with the increasing amount of Cys (Fig. 4C), and the ratio of two emission intensity (F_{405}/F_{640}) versus concentration of Cys was linear over the 0.1 μM - 50 μM (LOD = 0.04 μM; S/N = 3, Fig. 4D). Moreover, this novel method for the analysis of Hg^{2+} ions and Cys was compared with other methods. It showed high sensitivity and good linearity (As shown in the Table S1, S2, in the Supporting Information). In addition, the linear plots between F_{640} of as-prepared BSA-Pt-Au NCs and the concentrations of Hg^{2+} ions (Cys) were shown in Fig. S4. The results show that, compared with conventional detection method, the ratio-metric fluorescent detection technique has the higher sensitivity and wider linear range. Thus, a novel dual-emitting fluorescence sensor for the simultaneous detection of Hg^{2+} and Cys has been successfully constructed.

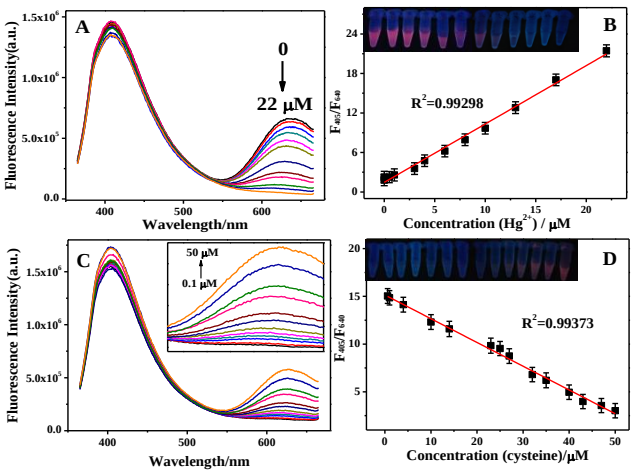

Fig. 4 (A) Fluorescence emission spectra of BSA-Pt-Au NCs in the presence of different concentrations of Hg^{2+} ions. (B) The fluorescence intensity ratio (F_{405}/F_{640}) of BSA-Pt-Au NCs in the presence of different concentrations of Hg^{2+} ions. (C) Fluorescence emission spectra of BSA-Pt-Au NCs in the presence of 22 μM Hg^{2+} ions and different concentrations of Cys. (D) The fluorescence intensity ratio (F_{405}/F_{640}) of BSA-Pt-Au NCs in the presence of 22 μM Hg^{2+} ions and different concentrations of Cys. The inset is the visual fluorescence images of various concentrations of Hg^{2+} ions and the mixtures of 22 μM Hg^{2+} ions with different concentrations of Cys in the BSA-Pt-Au NCs solution (from left to right).

Selectivity Studies

Considering the promise of the BSA-Pt-Au NCs sensor system for application in biological systems, to evaluate the selectivity of the fluorescence sensor for Hg^{2+} ions and Cys was indispensable. To investigate the selectivity of BSA-Pt-Au NCs to detect Hg^{2+} ions and Cys in aqueous solutions, different metal ions and the mixtures of Hg^{2+} ions with different amino acids were incubated with the BSA-Pt-Au NCs solution. From the Fig. 5A and 5B, as expected, the relatively ratio of fluorescence intensity (F_{405}/F_{640}) could trigger the immediate and significant quenching of the fluorescence of bimetallic BSA-Pt-Au NCs in the presence of Hg^{2+} ions, and recovery when the Hg^{2+} ions and Cys simultaneously exist. However, nearly negligible quenching or recovery was observed after adding other metal ions and amino acids into the bimetallic BSA-Pt-Au NCs solution, which is visibly shown in the corresponding fluorescence photographs (inset of Fig. 5A, 5B). The results demonstrate that the new sensing method is highly selective toward the Hg^{2+} ions and Cys and does not suffer from interference by the presence of all the other competitors.

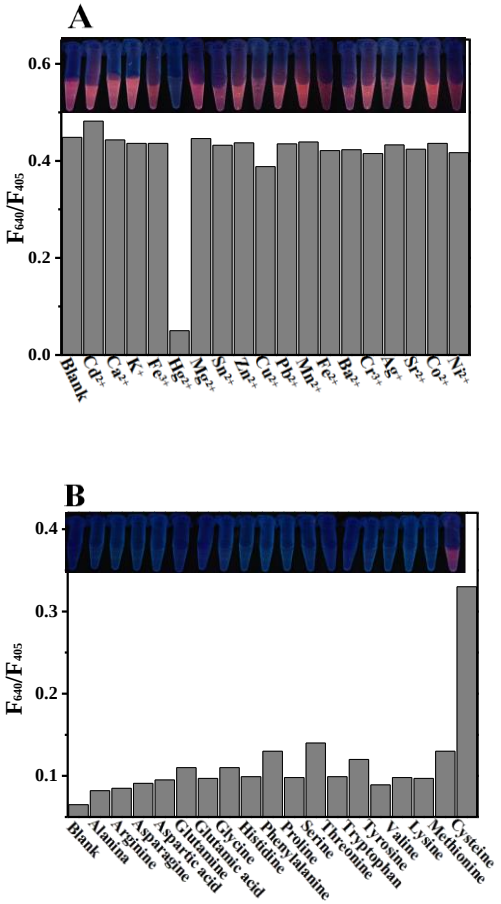

Fig. 5 Selectivity of BSA-Pt-Au NCs-based detection system. (A) The concentration of Hg^{2+} ions is 22 μM, but the concentrations of other ions are 50 μM. (B) The concentration of Cys is 50 μM, but the concentrations of other amino acids are 200 μM. The inset shows the corresponding photographs of visual fluorescence images of BSA-Pt-Au NCs with different metal ions and 22 μM Hg^{2+} ions with different amino acids under UV light.

Real Samples Testing

The developed dual-emitting fluorescence sensor was applied to the detection of Hg^{2+} and Cys in urine and serum samples. The

results are listed in Table S3 (Supporting Information), the recovery of the added amount of Hg^{2+} and Cys to the three different solutions for each sample was in the range of 99.4−102.5%, which indicates the proposed method possess excellent applicability for real sample analysis.

Conclusions

In summary, for the first time, bimetallic BSA-Au-Pt NCs with dual-emission (405 nm and 640 nm) fluorescence have been prepared through a one-pot synthetic strategy using the BSA as a template under alkaline conditions. The emission intensity at 640 nm decreases dramatically with addition of Hg^{2+} ions based on the specific and strong d^{10}-d^{10} interaction between Hg^{2+} ions and Au atoms/ions and recoveries after introducing the Cys due to the strong interaction between Hg^{2+} ions and thiol functional group. As far as we know, this is the first fluorescence ratio-metric method to measure Hg^{2+} ions and Cys based on the fluorescence intensity ratios (F_{405}/F_{640}) related to the concentrations of Hg^{2+} ions (Cys). The developed nanosensor shows high sensitivity and selectivity, which is superior to most current approaches analysis. And the dual-emitting BSA-Au-Pt NCs may be good potential candidates for further applications in bioimaging, biosensing and catalysis.

Associated Content

*S Supporting Information

Additional information as noted in the text, including one figure and two tables.

Acknowledgements

S.-N. Ding and Y.-X. Guo contributed equally to this work. This work was supported by the National High Technology Research and Development Program ("863" Program) of China (2015AA020502), the Open Research Fund of State Key Laboratory of Bioelectronics, Southeast University, and the Open Research Fund of Key Laboratory of Energy Thermal Conversion and Control of Ministry of Education, Southeast University.

Notes and reference

1. W. de Vries, P. F. A. M. Romkens and G. Schuetze, *Rev Environ Contam Toxicol*, 2007, **191**, 91-130.
2. L. Shang, L. Yang, F. Stockmar, R. Popescu, V. Trouillet, M. Bruns, D. Gerthsen and G. U. Nienhaus, *Nanoscale*, 2012, **4**, 4155-4160.
3. J. Liu, X. L. Ren, X. W. Meng, Z. Fang and F. Q. Tang, *Nanoscale*, 2013, **5**, 10022-10028.
4. D. Mergler, H. A. Anderson, L. H. M. Chan and K. R. Mahaffey, *Neuroendocrinol. Lett.*, 2007, **36**, 3-11.
5. F. Zahir, S. J. Rizwi, S. K. Haq and R. H. Khan, *Environ. Toxicol. Phar.*, 2005, **20**, 351-360.
6. J. V. Cizdziel and S. Gerstenberger, *Talanta*, 2004, 64, 918-921.
7. Z. Zhu, Y. Su, J. Li, D. Li, J. Zhang, S. Song, Y. Zhao, G. Li and C. Fan, *Anal. Chem.*, 2009, **81**, 7660-7666.
8. Dingbin Liu, Weisi Qu, Wenwen Chen, Wei Zhang, Zhuo Wang and X. Jiang, *Anal. Chem.*, 2010, **82**, 9606-9610.
9. Z. Sun, N. Zhang, Y. Si, S. Li, J. Wen, X. Zhu and H. Wang, *Chem. Commun.*, 2014, **50**, 9196-9199.
10. S. C. K. Shum, H. M. Pang and R. S. Houk, *Anal. Chem.*, 1992, **64**, 2444-2450.
11. G. S. Anand, A. I. Gopalan, S.-W. Kang and K.-P. Lee, *J. Anal. Atom. Spectrom.*, 2013, **28**, 488.
12. S. Chen, D. Liu, Z. Wang, X. Sun, D. Cui and X. Chen, *Nanoscale*, 2013, **5**, 6731-6735.
13. D. Lu, C. Zhang, L. Fan, H. Wu, S. Shuang and C. Dong, *Analytical Methods*, 2013, **5**, 5522.
14. X. Yuan, T. J. Yeow, Q. B. Zhang, J. Y. Lee and J. Xie, *Nanoscale*, 2012, **4**, 1968-1971.
15. H. Xu, X. Zhu, H. Ye, L. Yu, X. Liu and G. Chen, *Chem. Commun.*, 2011, **47**, 12158-12160.
16. M. T. Heafield, S. Fearn, G. B. Steventon, R. H. Waring, A. C. Williams and S. G. Sturman, *Neurosci. Lett.*, 1990, **110**, 216-220.
17. X. N. Cao, J. H. Li, H. H. Xu, L. Lin, Y. Z. Xian, K. Yamamoto and L. T. Jin, *Biomed. chromatogr. : BMC*, 2004, **18**, 564-569.
18. G. Chen, L. Zhang and J. Wang, *Talanta*, 2004, **64**, 1018-1023.
19. N. Burford, M. D. Eelman, D. E. Mahony and M. Morash, *Chem. Commun.*, 2003, 146-147.
20. Y. W. Lin, C. C. Huang and H. T. Chang, *The Analyst*, 2011, **136**, 863-871.
21. Y. L. Wang, Chen J.J. and J. Irudayaraj, *ACS Nano*, 2011, **5**, 9718-9725.
22. J. P. Xie, Y. G. Zheng and J. Y. Ying, *J. Am. Chem. Soc.*, 2009, **131**, 888-889.
23. H. Wei, Z. Wang, L. Yang, S. Tian, C. Hou and Y. Lu, *The Analyst*, 2010, **135**, 1406.
24. C. Sun, H. Yang, Y. Yuan, X. Tian, L. Wang, Y. Guo, L. Xu, J. Lei, N. Gao, G. J. Anderson, X. J. Liang, C. Chen, Y. Zhao and G. Nie, *J. Am. Chem. Soc.*, 2011, **133**, 8617-8624.
25. T. H. Chen, C. Y. Lu and W. L. Tseng, *Talanta*, 2013, 117, 258-262.
26. P. Pyykko, *Angew. Chem. Int. Ed. Engl.*, 2004, **43**, 4412-4456.
27. J. Xie, Y. Zheng and J. Y. Ying, *Chem. Commun.*, 2010, **46**,961-963.
28. C. Katherine, R. G. F. Grabar, B. H. Michael and M. J. Natan, *Anal. Chem.*, 1995, **67**, 735-743.
29. Y. N. Chen, P. C. Chen, C. W. Wang, Y. S. Lin, C. M. Ou, L. C. Ho and H. T. Chang, *Chem. Commun.*, 2014, **50**, 8571-8574.
30. T. G. Huggins, M. C. Wells-Knecht, N. A. Detorie, J. W. Baynes, S. R. Thorpe, *Biological Chemical*, 1993, **268**, 12341-12347.
31. K. Severin, R. Bergs and W. Beck, *Angew. Chem. Int. Ed.*, 1998, **37**, 1634-1654.
32. H. X. Zhao, L. Q. Liu, Z. D. Liu, Y. Wang, X. J. Zhao and C. Z. Huang, *Chem. Commun.*, 2011, **47**, 2604-2606.
33. S. L. Raut, R. Fudala, R. Rich, R. A. Kokate, R. Chib, Z. Gryczynski, I. Gryczynski, *Nanoscale*, 2014, **6**, 2594-2597.
34. X. Wang, L. Cao, F. Lu, M. J. Meziani, H. Li, G. Qi, B. Zhou, B. A. Harruff, F. Kermarrec and Y. P. Sun, *Chem. Commun.*, 2009, **25**, 3774-3776.
35. H. Zhang, Y. Li, X. Liu, P. Liu, Y. Wang, T. An, H. Yang, D. Jing and H. Zhao, *Environ. Sci. & Technol.*, 2014, **1**, 87-91.
36. K. P. Gong, F. Du, Z. H. Xia, M. Durstock and L. M. Dai1, *SCIENCE*, 2009, 323.
37. Z. X. Wang and S. N. Ding, *Anal. Chem.*, 2014, **86**, 7436-7445.